IGFBP5 induces cell adhesion, increases cell survival and inhibits cell migration in MCF-7 human breast cancer cells

Angara Sureshbabu[1], Hiroshi Okajima[2], Daisuke Yamanaka[2], Elizabeth Tonner[1], Surya Shastri[1], Joanna Maycock[3], Malgorzata Szymanowska[1], John Shand[1], Shin-Ichiro Takahashi[2], James Beattie[3], Gordon Allan[1] and David Flint[1,*]

[1]Strathclyde Institute of Pharmacy and Biomedical Sciences, University of Strathclyde, 161 Cathedral Street, Glasgow, G4 0RE, United Kingdom
[2]Graduate School of Agriculture and Life Sciences, University of Tokyo, 1-1-1, Yayoi, Bunkyo-ku, Tokyo, 113-8657, Japan
[3]Department of Oral Biology, Leeds Dental Institute, University of Leeds, Clarendon Way, Leeds, LS2 9LU, United Kingdom
*Author for correspondence (david.flint@strath.ac.uk)

Accepted 9 December 2011
Journal of Cell Science 125, 1693–1705

doi: 10.1242/jcs.092882

Summary

Maintenance of tissue boundaries is crucial for control of metastasis. We describe a new signalling pathway in which epithelial cell disruption can be minimised and thereby restricts epithelial–mesenchymal transgressions. This involves the release of insulin-like growth factor (IGF)-binding protein 5 (IGFBP5) from apoptotic cells, which increases the adhesion of epithelial cells on mesenchymal but not epithelial extracellular matrix (ECM), and involves the direct interaction of IGFBP5 and α2β1 integrins. IGFBP5 also induced cell adhesion to vitronectin in the absence of αVβ3 integrin, the vitronectin receptor, again through an α2β1-integrin-dependent action, suggesting that IGFBP5 can induce spreading on matrices, even in the absence of the integrins normally used in this process. Using IGFBP5 mutants we demonstrate that the effect is IGF-independent but requires the heparin-binding domain in the C-terminus of IGFBP5. A truncated mutant containing only the C-terminal of IGFBP5 also induced adhesion. Adhesion induced by IGFBP5 was dependent on Cdc42 and resulted in activation of integrin-linked kinase (ILK) and Akt. Consistent with these changes, IGFBP5 facilitated prolonged cell survival in nutrient-poor conditions and decreased phosphorylation of the stress-activated kinase p38 MAPK (MAPK14). Whereas IGFBP5 enhanced adhesion, it inhibited cell migration, although this was not evident using the truncated C-terminal mutant, suggesting that effects of IGFBP5 on adhesion and migration involve different mechanisms. We anticipate that these responses to IGFBP5 would reduce the metastatic potential of cells.

Key words: IGFBP5, Integrin, Adhesion, Survival, Migration

Introduction

Formation of morphological boundaries within tissues is required to achieve the segregation of cells into separate populations. Once formed, boundaries must be maintained, despite being subjected to a range of traumatic insults, such as metastasis, where epithelial cells migrate through mesenchymal tissues and across endothelial barriers to new sites in the body.

Recently, several studies have linked insulin-like growth factor (IGF)-binding protein 5 (IGFBP5) to metastasis. For example, increased IGFBP5 expression has been associated with poor prognosis during metastasis (Pekonen et al., 1992; McGuire et al., 1994; Huynh, 1998; Mita et al., 2007). By contrast, we have shown that, at high concentrations, IGFBP5 is apoptotic in mammary gland epithelial cells both in vitro and in vivo (Tonner et al., 2002; Marshman et al., 2003) and is the only IGFBP whose levels increase dramatically during involution of the mammary gland (Clarkson and Watson, 2003; Stein et al., 2004). Consistent with this apoptotic role, decreased expression of IGFBP5 is associated with increased tumorigenesis in osteosarcoma (Su et al., 2011) and in breast cancer after foetal alcohol exposure (Polanco et al., 2010). Furthermore, overexpression of IGFBP5 has been shown to inhibit MCF-7 breast cancer cell tumour growth in vivo, and increased expression of IGFBP5 has been shown to be associated with increased survival of breast cancer patients (Ahn et al., 2010).

Despite the increasing number of studies supporting a role for IGFBP5 in tumorigenesis and metastasis, few studies have provided any mechanistic insights. In order to clarify the role of IGFBP5 in mammary metastasis, we investigated the actions of IGFBP5 on MCF-7 cells and provide evidence to demonstrate that IGFBP5 enhances responses that maintain the integrity of the epithelial–mesenchymal boundary. As such, IGFBP5 might have a central role in limiting metastasis.

We demonstrate, for the first time, that these effects of IGFBP5 are IGF-independent but are dependent upon Cdc42 activation and a direct interaction with α2β1 integrins that leads to activation of Akt on Ser473. This pathway normally leads to both proliferation and migration signals, the latter through activation of focal adhesion kinase (FAK) (Wang and Basson, 2009). However, IGFBP5 induced sustained phosphorylation of p53, which is known to inhibit activation of FAK (Cance and Golubovskaya, 2008), and, consistent with this, IGFBP5 prevented migration of MCF-7 cells. We propose that these actions of IGFBP5 lead to an adhesive, anti-migratory and pro-survival epithelial phenotype,

which could serve to limit a variety of epithelial–mesenchymal transgressions.

Results

MCF-7 cells, when cultured in serum-free conditions, showed weak adhesion to the substratum and, instead, formed multicellular spheroids (Fig. 1A). Treatment with IGFBP5 apparently decreased cell–cell contact and promoted cell adhesion to the substratum. When individual cells attached to the substratum under the influence of IGFBP5, they did so with three- or four-point attachments using focal adhesions, which could be visualised with paxillin (Fig. 1B, left panel). This adhesion was reminiscent of Cdc42-activated adhesion (Hall, 1998) and distinct from that induced by serum (Fig. 1B, right panel). In contrast to the results upon treatment with IGFBP5, IGF1 increased migration of cells and led to the production of larger 'spheroids' in which plasma membrane expression of E-cadherin was further upregulated (Fig. 1C). Although IGFBP5 appeared to enhance disruption of spheroids, in fact this was not the case because, although cells attached to the substratum, they retained their epithelial characteristics and showed abundant expression of E-cadherin at the plasma membrane (Fig. 1C). This result suggests that IGFBP5 application induces alterations in cell-surface interactions with the extracellular matrix (ECM), while cell–cell contact is retained. We therefore compared the ability of IGFBP5 to induce cellular attachment to various ECM components: collagen, fibronectin, laminin, vitronectin and fibrin. The potency of IGFBP5 was evident in the presence of collagen, fibronectin, vitronectin and fibrin, but it was greatly reduced in the presence of laminin (Fig. 1D). This effect of IGFBP5 was confirmed in studies where cells were transfected with an adenovirus expressing IGFBP5 (Fig. 1E). The effects of IGFBP5 took a little longer to appear (48–72 hours), but this probably reflects the time taken for IGFBP5 to accumulate in the medium. During these cultures, IGFBP5 concentrations reached ~50–200 ng/ml, as determined by ELISA (results not shown).

Although these results suggest that there is an IGF-independent action of IGFBP5, it was conceivable that endogenous production of IGF1 or IGF2 by MCF-7 cells had been inhibited by IGFBP5. To address this possibility we repeated the experiment using

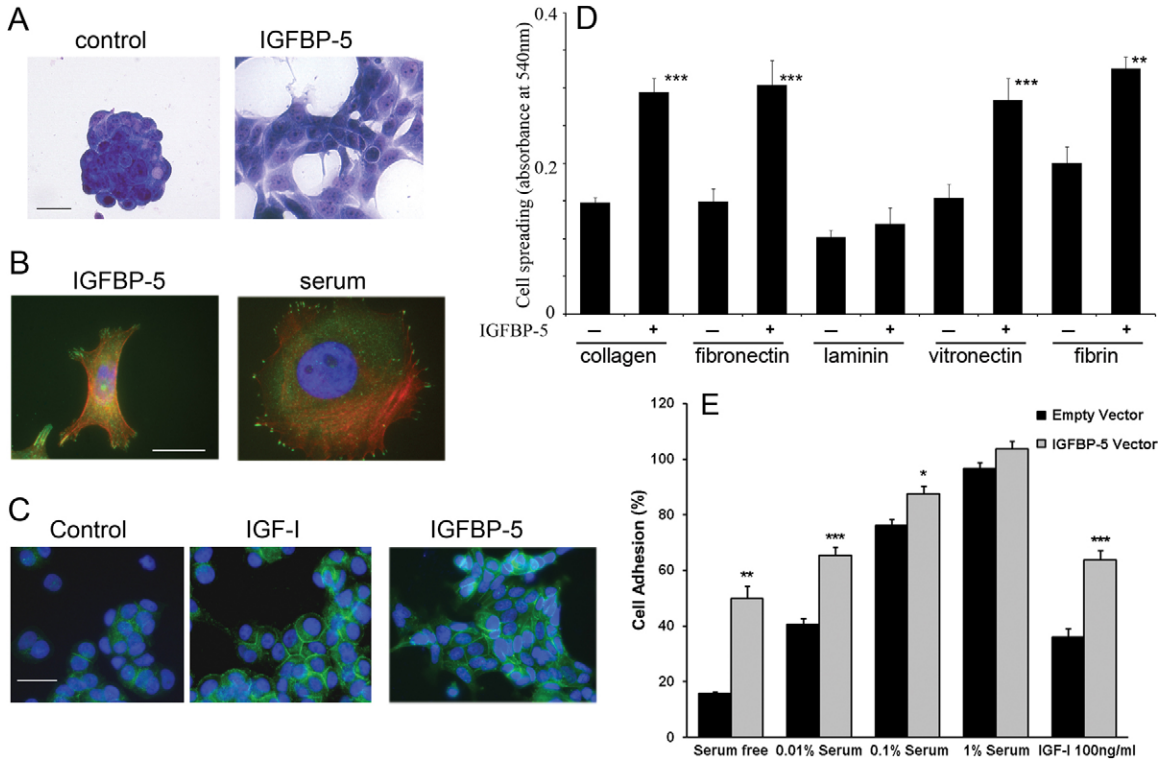

Fig. 1. IGFBP5 induces adhesion to mesenchymal and provisional matrices but not to basement membrane. (**A**) MCF-7 cells cultured in serum-free medium for 24 hours form multicellular spheroids. IGFBP5 (10 µg/ml) induces dissolution of the spheroid, involving spreading onto the substratum. Cells were stained with Crystal Violet. (**B**) Where individual cells attached, it involved a characteristic three- or four-point contact and these focal adhesions possessed abundant paxillin (green). This contrasts with the adhesion induced by serum, where cells show uniform spreading across the cell and become much flatter with a far greater cytoplasmic and nuclear area. (**C**) Treatment for 24 hours with IGF1 (IGF-I, 100 ng/ml) stimulated the formation of larger spheroids and enhanced the expression of E-cadherin (green). Although IGFBP5 (10 µg/ml) induced cell adhesion to the substratum, these cells also maintained a strong E-cadherin expression. (**D**) IGFBP5-induced adhesion was clearly evident in the presence of collagen, fibronectin, vitronectin and fibrin but was inhibited in the presence of laminin. MCF-7 cells were cultured in serum-free conditions for 24 hours in the presence or absence of IGFBP5 (10 µg/ml) after which cells were fixed with 4% PFA and stained with Crystal Violet. Absorbances were determined at 540 nm. Values are means+s.e.m. (n=3–9). $^{**}P<0.01$, $^{***}P<0.001$ compared with control (ANOVA followed by Bonferroni's post-hoc test). (**E**) IGFBP5 expressed though adenovirus transfection also increased MCF-7 cell adhesion. Cells were infected with Ad-IGFBP5 or Ad-null virus at 200 MOI. Cells were then trypsinised and seeded into 96-well plates in various concentrations of serum, with or without IGF1 (100 ng/ml). After 3 days cells were fixed, stained with Crystal Violet and absorbances determined as described in the Materials and Methods. Values are means+s.e.m. (n=12). $^{*}P<0.05$, $^{**}P<0.01$, $^{***}P<0.001$ compared with control (ANOVA followed by Bonferroni's post-hoc test). Scale bars: 25 µm.

mutant forms of IGFBP5. One mutant (N-term) was designed to remove the ability to bind to IGFs, whereas a second (C-term) had all of the basic residues in the heparin-binding domain mutated (Fig. 2). The effect of IGFBP5 on cell spreading was evident in the N-term mutant which does not bind to IGF1, but was lost in the C-term mutant in which the heparin-binding domain of IGFBP5 had been mutated (Fig. 3A,B), demonstrating that the effect of IGFBP5 is IGF-independent but requires the heparin-binding domain. Furthermore, a mutant IGFBP5, comprising only the C-terminal domain of IGFBP5, also induced cell adhesion (Fig. 3C,D).

To assess the biological relevance of this adhesion event we first examined the effects of IGFBP5 on cell survival when the cells were stressed, by culture in serum-free medium in the absence of medium changes. The ability of IGFBP5 to induce adhesion was accompanied by increased cell survival in such nutrient-deprived conditions. When seeded at high density, in serum-free conditions, control cells did not adhere well and detached within 2–5 days (Fig. 4A,B). By contrast, in the presence of IGFBP5 cell adhesion increased and cell numbers remained significantly higher than in the controls for at least 9 days. Assessment of cell viability clearly demonstrated that, when cells were seeded at high cell density, live cell numbers declined dramatically between days 6–10 in controls but this did not occur in IGFBP5-treated cells until days 12–14 (Fig. 4C). Conversely, dead cell numbers increased by day 6, peaking at day 8 in controls (Fig. 4D), whereas this was delayed by ~4 days in IGFBP5-treated cells.

In order to begin to understand the mechanism of this survival action of IGFBP5, we undertook a systematic study of the major pathways typically involved, including integrins, small GTPases and intracellular kinases. Integrins are important adhesion molecules and we therefore examined the effect of IGFBP5 on cell-surface expression of integrins, using an α- and β-integrin-binding cell adhesion assay based upon cell capture by monoclonal antibodies raised against a panel of integrins. To our surprise, rather than increasing integrin expression, IGFBP5 induced modest but significant decreases in α5-, β1- and αvβ5 integrins (Fig. 5A,B). These changes in integrin expression clearly did not explain the increased adhesion induced by IGFBP5 but, by using a series of function-blocking antibodies to various integrins, we showed that the actions of IGFBP5 were inhibited by function-blocking antibodies to α2 and β1 integrins as well as (to a lesser extent) by those against αvβ6 (Fig. 5C). Because IGFBP5 had also been shown to induce adhesion to vitronectin (a β3 integrin binder), we examined the ability of function-blocking antibodies to disrupt this interaction. Surprisingly, the action of IGFBP5 was again inhibited by antibodies which blocked α2 and β1 integrins but not by those targeting the classical αvβ3 integrin (Fig. 5D). Given that IGFBP5 induced adhesion without increasing integrin expression on the cell surface, and that its effect was α2β1 integrin-dependent, we used biosensor analysis to examine the possibility that IGFBP5 interacted directly with α2β1 integrins. Fig. 5E clearly shows that α2β1 integrin in solution binds to immobilised IGFBP5. Binding occurred in a concentration-dependent manner and was linear during the association phase for each concentration of integrin. Dissociation of IGFBP5–integrin complexes appeared to be very slow, suggesting that this was a stable complex. Sensorgrams fitted well using a 1:1 Langmuir binding model reporting an association rate ($K_a = 1.7 \times 10^5\ M^{-1}s^{-1}$) and dissociation rate constant ($K_d = 9.3 \times 10^{-5}\ s^{-1}$). This suggests that there is a tight binding complex between IGFBP5 and α2β1 integrin, with an equilibrium constant of ~0.5 nM, suggesting that it is physiologically relevant. IGFBP5 also bound to α2β1 integrin after mutation of either the N-terminal IGF-binding site or the heparin-binding domain in the C-terminus (Fig. 5F). Consistent with the ability of IGFBP5 to induce adhesion through an integrin-dependent mechanism, IGFBP5 increased the expression of ILK, either after exogenous addition of IGFBP5 or after transfection with adenovirus containing IGFBP5 (Fig. 6).

The intracellular mechanisms involved in IGFBP5 actions are not well understood and we therefore examined the effects of IGFBP5 on cell adhesion using various kinase inhibitors and western blotting. LY-294002, an inhibitor of the phosphoinositide 3-kinase (PI3K) pathway, PD98059, an inhibitor of MAP kinase kinases (also known as MAPK/ERK kinases or MEKs), and UO126, an inhibitor of ERK1/2 activation, had no effect on cell adhesion, either alone or in combination with IGFBP5 (Fig. 7). By contrast, SB203580, an inhibitor of p38 MAPK (MAPK14), A8301 and SB413542 (both inhibitors of SMAD pathways) actually significantly enhanced the actions of IGFBP5. To characterise further the intracellular responses to IGFBP5, we used a commercial kinase array representing 42 different phosphorylation sites on 37 different kinases and identified several significant changes in response to IGFBP5 treatment. After 6 hours, IGFBP5 induced a decrease in phosphorylation of p38 MAPK (Fig. 8A). This was consistent with the increased adhesion, which was evident when p38 MAPK

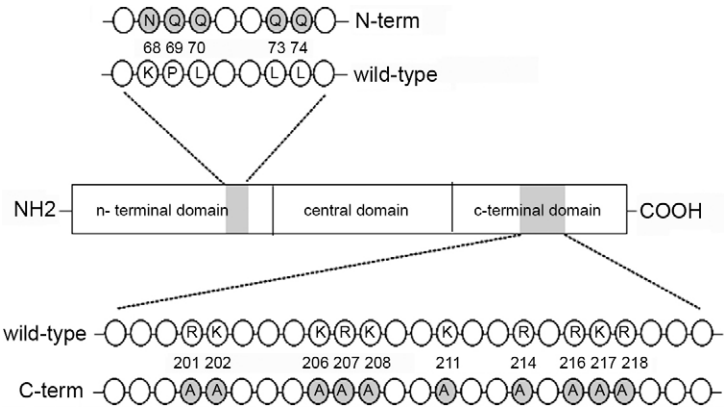

Fig. 2. Representation of mutations performed to generate an IGFBP5 mutant that does not bind to IGFs (N-term) and a mutant that does not bind to heparin (C-term).

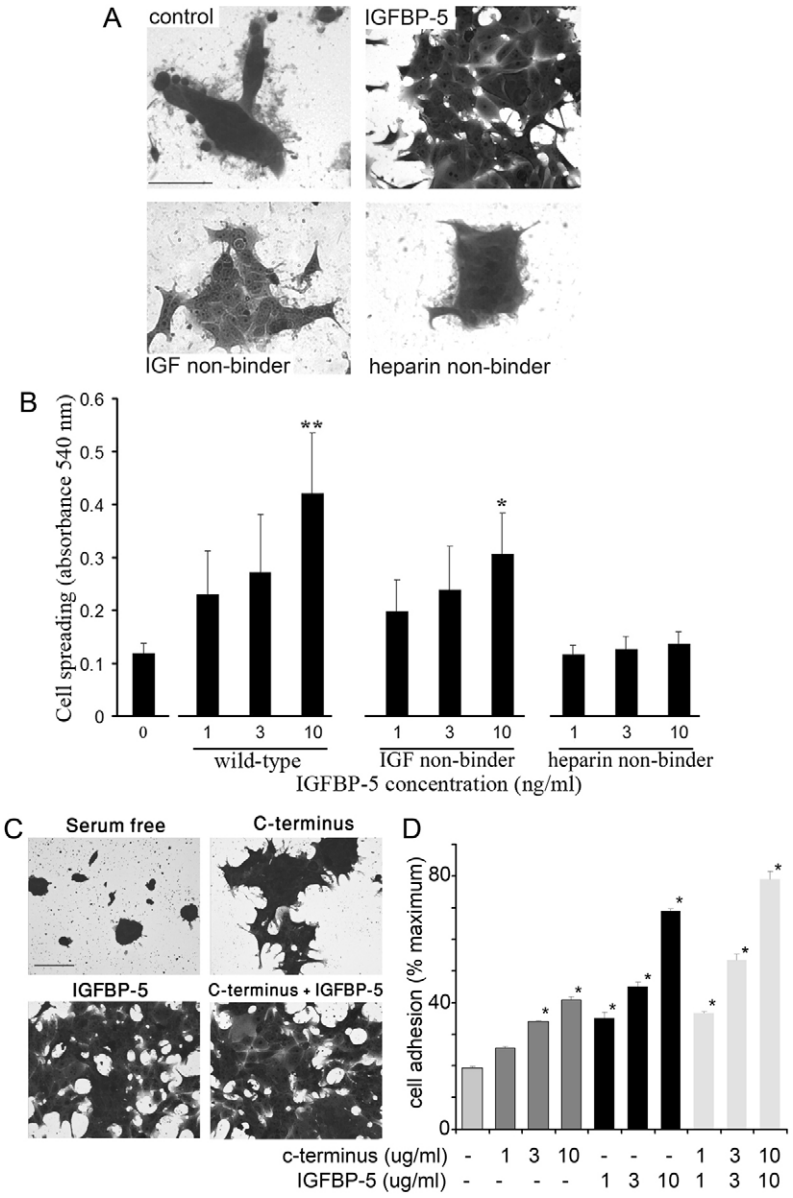

Fig. 3. Adhesion induced by IGFBP5 is IGF-independent but requires the heparin-binding domain. (**A**) IGFBP5 induces cell adhesion, as does a mutant IGFBP5 (N-term) which does not bind IGF1 or IGF2 (IGF non-binder). By contrast, a mutant that does not bind to heparin (C-term) does not induce cell adhesion. Cells were cultured in serum-free conditions for 24 hours in the presence or absence of wild-type or mutant IGFBP5 (10 μg/ml) after which they were fixed and stained with Crystal Violet and absorbances determined at 540 nm. (**B**) Absorbance values for experiment described in A. Values are means+s.e.m. (n=4–5). *P<0.05, **P<0.01 compared with control (ANOVA followed by Bonferroni's post-hoc test). (**C**) The C-terminus of IGFBP5 induces cell adhesion. Cells were cultured for 24 hour in the presence or absence of IGFBP5 (10 μg/ml) or the C-terminus of IGFBP5 (10 μg/ml). Cells were fixed and stained. (**D**) Absorbance values for study described in C. Values are means+s.e.m. (n=6). *P<0.01 compared with control (ANOVA followed by Bonferroni's post-hoc test). Scale bars: 50 μm.

was inhibited using SB203580 (Fig. 7). IGFBP5 also induced a 2.5-fold increase in phosphorylation of p53 on S392 and a 2-fold increase on S46, although S15 was unaffected. After 48 hours, increased phosphorylation of p53 (S392) was still evident and these results were confirmed using standard western blotting techniques (Fig. 8C). There was also a dramatic 5-fold increase in phosphorylation of Akt on S473 but not on S308, although S308 was clearly phosphorylated (Fig. 8B). This phosphorylation pattern for Akt is consistent with activation through an integrin-linked pathway and/or mammalian target of rapamycin (mTOR), rather than PI3K, which is classically associated with phosphorylation of S308. However, we found no evidence of activation of mTOR and thus our results suggest an integrin-mediated activation of this survival and proliferation pathway. In order to confirm that the increased phosphorylation of S473 translated into a true activation of Akt, activity assays were performed; these confirmed that Akt activity was increased at both 24 hours and 48 hours after IGFBP5 treatment (Fig. 8D). Despite activating Akt (a stimulus that leads to FAK phosphorylation and cell migration), IGFBP5 did not induce FAK activation (Fig. 8A,B).

In order to characterise further the nature of the adhesion process, we examined the role of the small GTPases, Rho, Rac and Cdc42 in the action of IGFBP5 on MCF-7 cells. MCF-7 cells were infected with dominant negative (DN) Rho, Rac, Cdc42 or null adenovirus. Effectiveness of the infections was assessed by attempting to activate the GTPases with GTPγS. Although there was abundant Rho protein in the cells, GTPγS only weakly activated Rho in serum-free conditions, although DN Rho appeared to completely inhibit this modest activation (Fig. 9A). Rac and Cdc42 were clearly activated by GTPγS in cells infected with null virus, and again this was markedly attenuated in the DN Rac and DN Cdc42 cells, respectively. We were unable to demonstrate activation of any of these GTPases by IGFBP5 under similar conditions, although this might simply reflect a lack of sensitivity in the assay in serum-free conditions (results not

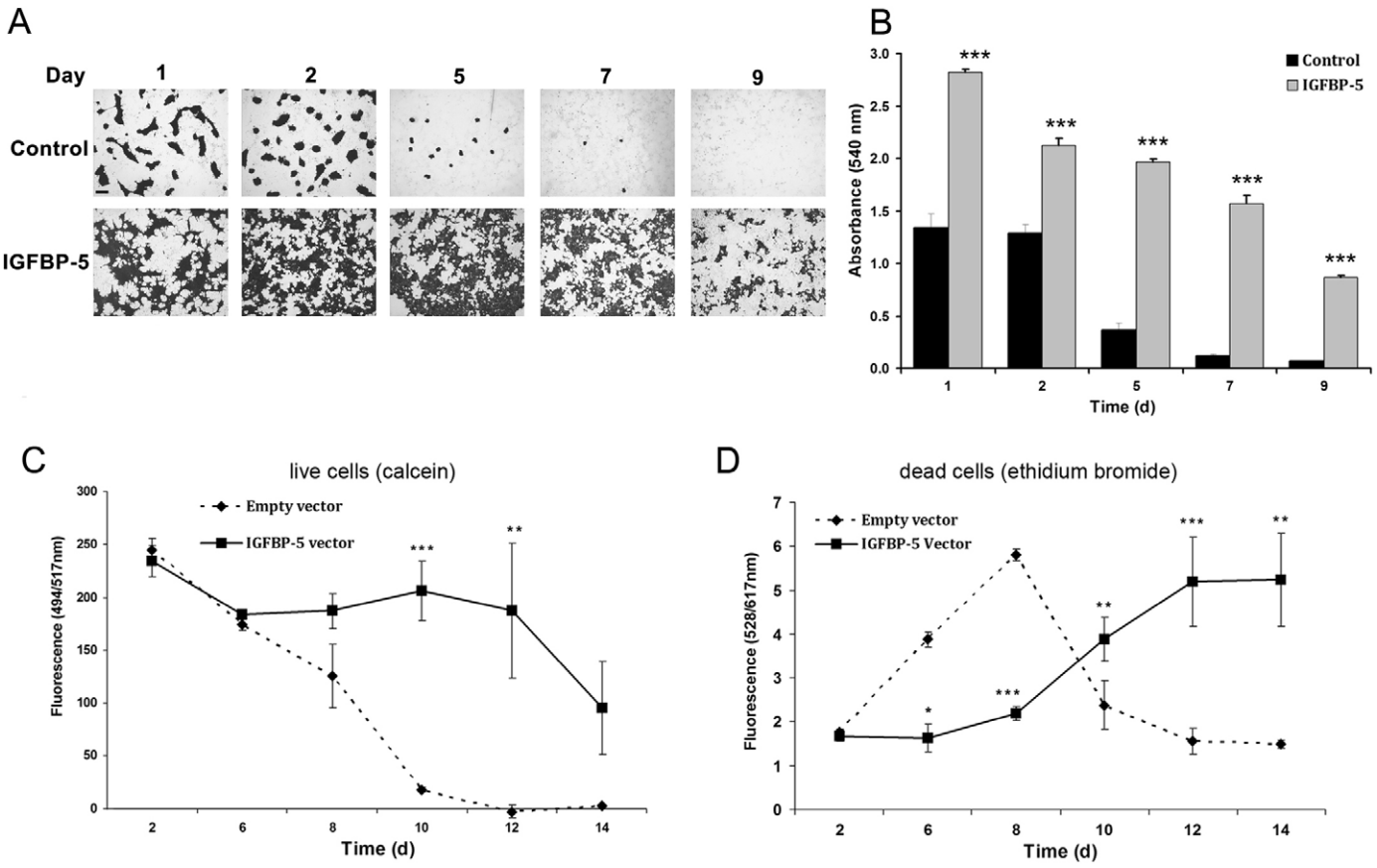

Fig. 4. IGFBP5 enhances cell survival. (**A**) MCF-7 cells were seeded at high density (5×10^4 cells per well) in serum-free conditions with or without the addition of 10 μg/ml of exogenous IGFBP5. Scale bar: 100 μm. At various time intervals cells were fixed and stained with Crystal Violet. (**B**) Absorbance values for Crystal Violet staining were determined for cells in A. Values are means+s.e.m. ($n=6$). ***$P<0.001$ compared with control (ANOVA followed by Bonferroni's post-hoc test). Cells seeded at high density (5×10^4 cells per well) were also incubated with cell viability stain and live (**C**) and dead cell (**D**) fluorescence values were determined as described in the Materials and Methods section. Values are means ± s.e.m. ($n=6$). *$P<0.05$, **$P<0.01$, ***$P<0.001$ compared with control (ANOVA followed by Bonferroni's post-hoc test).

shown). Notwithstanding this limitation, IGFBP5 induced cell adhesion in the presence of DN Rho and DN Rac, whereas, in the presence of DN Cdc42, its actions were attenuated (Fig. 9B–D). This finding supported the conclusions from the phenotypic appearance of the adhesion process, which was consistent with a Cdc42-mediated process (Hall, 1998).

Despite the increase in cell adhesion, IGFBP5 significantly inhibited, rather than stimulated, migration of MCF-7 cells in response to three potent stimuli, IGF1, EGF and serum (Fig. 10A–C). Furthermore, the effect of IGFBP5 was shown to be IGF-independent because a mutant that could not bind to IGFs (N-term), potently inhibited cell migration, whereas a mutant which could not bind to heparin through its C-terminus (C-term) was inactive (Fig. 10D,E). Despite the fact that the C-terminal heparin-binding domain is essential for the inhibition of migration, a mutant consisting exclusively of the C-terminal domain, and thus containing the heparin-binding domain, failed to influence cell migration (Fig. 10F,G) even though it was able to induce adhesion (Fig. 3). This suggests that the heparin-binding domain is necessary but not sufficient to inhibit migration.

When we examined wound edges, it was evident that IGFBP5-treated cells maintained E-cadherin expression up to and including the cells at the wound edge (Fig. 11), and these cells also retained F-actin expression in an epithelial pattern (note the alignment of F-actin along the wound edge). By contrast, in control cells, E-cadherin expression decreased at the wound edge as cells had reorganised actin stress fibres and underwent migration (note the actin organisation in the lamellipodia of several control cells). There were abundant focal adhesions, as judged by paxillin expression in both control and IGFBP5-treated cells (Fig. 11).

Finally, we examined gene expression using a targeted array of 84 genes associated with the ECM and/or adhesion. Three arrays with independent samples were analysed. Only three genes were consistently influenced by IGFBP5; these were decreases in *COL7A1* (encoding the collagen VII α1 chain) by 47%, *MMP1* (matrix metalloproteinase-1) by 66% and *MMP2* by 47%.

Discussion

We have identified a new role for IGFBP5 in the induction of cell adhesion and spreading that could have an important role in the prevention of metastasis. This adhesion was driven by the presence of collagen or fibronectin, components of the mesenchymal matrix, as well as vitronectin and fibrin (which are present as part of the wound healing response), but was

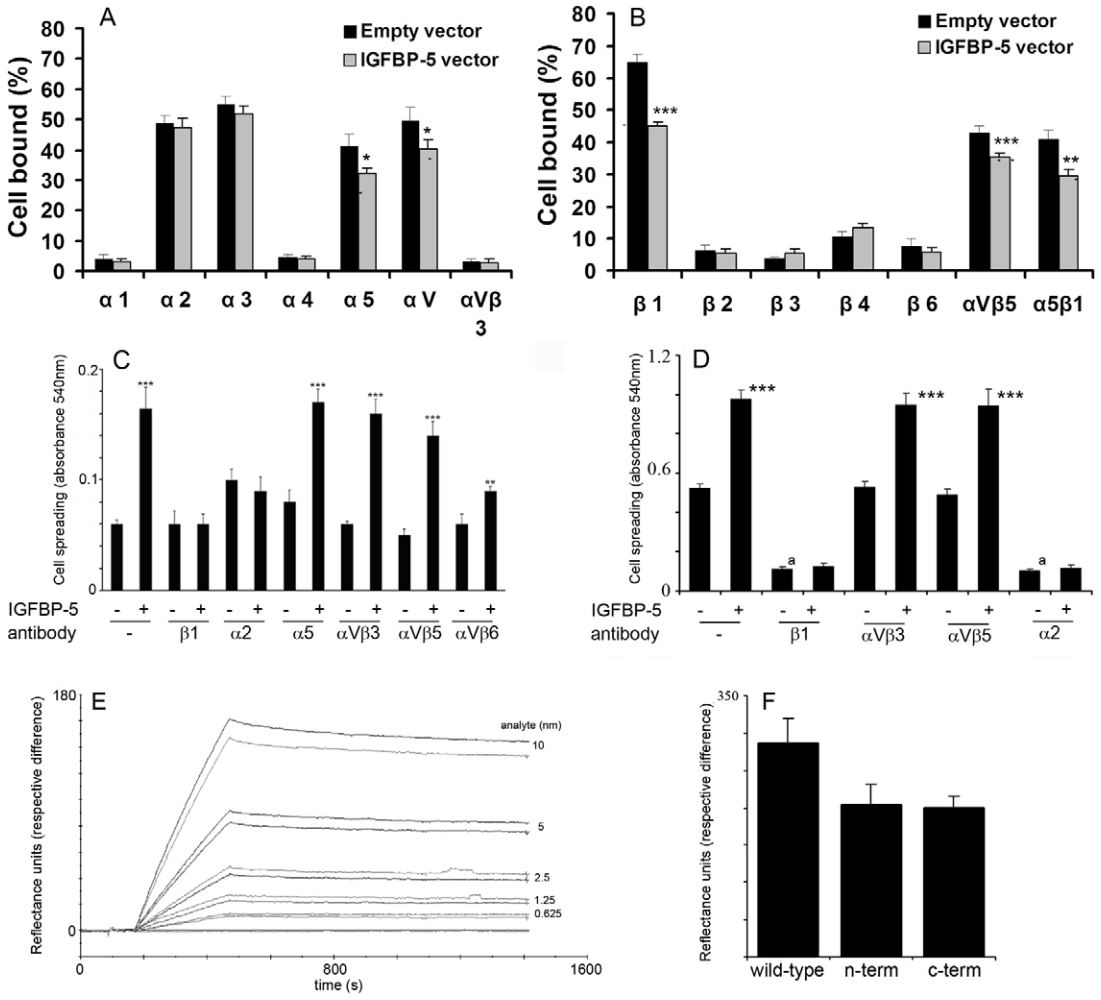

Fig. 5. Cell-surface integrin levels in MCF-7 cells. (**A**) α-integrin expression, and (**B**) β-integrin expression in MCF-7 cells that were transfected with Ad-IGFBP5 or Ad-null adenovirus for 48 hours. Cells were trypsinised and seeded (5×10^4 cells per well) into 96-well strips containing various antibodies against integrins. After 3 hours cells were washed to remove unbound cells, fixed and stained and absorbances determined. Values are means+s.e.m. ($n=6$). $^*P<0.05$, $^{**}P<0.01$, $^{***}P<0.001$ compared with control (ANOVA followed by Bonnferroni's post-hoc test). (**C**) Inhibition of IGFBP5-mediated cell adhesion by function-blocking integrin antibodies. MCF-7 cells were trypsinised and added to 96-well plates in 0.1% BSA in DMEM in the presence or absence of IGFBP5 (10 μg/ml) and function-blocking antibodies to integrins (30 μg/ml). After 18 hours, cells were fixed and stained with Crystal Violet and absorbances determined at 540 nm. Values are means+s.e.m. ($n=6$–8). $^{**}P<0.01$, $^{***}P<0.001$ compared with control (ANOVA followed by Bonferroni's post-hoc test). (**D**) Inhibition of IGFBP5-mediated cell adhesion by function-blocking integrin antibodies on vitronectin-coated plates. Plates were coated with 1 μg/ml vitronectin for 1 hour and then washed to remove unbound material. Cell adhesion was then performed as in C. Values are means+s.e.m. ($n=5$). $^{**}P<0.01$, $^{***}P<0.001$, compared with control, $^{a}P<0.05$ compared with no antibody control (ANOVA followed by Bonnferroni's post-hoc test). (**E**) Biosensor analysis of the interaction between immobilised IGFBP5 and α2β1 integrin. α2β1 integrin binding was analysed by random injection in duplicate at concentrations of 0, 0.625, 1.25, 2.5, 5 and 10 nM. Sensorgrams were fitted with the 1:1 Langmuir binding model provided in the instrument software. (**F**) Biosensor analysis of the interaction between immobilised IGFBP5 (wild-type or mutants) and 10 nM α2β1 integrin. Values are means+s.e.m. ($n=7$). Statistical analysis (ANOVA) revealed no significant differences.

limited in the presence of laminin, the major component of the epithelial basement membrane. Thus, this action of IGFBP5 would only be expected to occur during exposure of epithelial cells to a mesenchymal environment such as occurs during metastasis when epithelial–mesenchymal boundaries are compromised. Similar alterations to the response of both IGFBP3 and IGFBP5 in the presence of laminin or fibronectin have been described previously (McCaig et al., 2002).

Activation of the mesenchymal compartment, while the epithelial–mesenchymal boundary is maintained, is also evident in the mammary gland during the involution that occurs at the end of lactation. Despite huge increases in the expression of matrix metalloproteases, which aid in epithelial cell death (Tonner et al., 1997; Clarkson and Watson, 2003; Stein et al., 2004), many ductal cells survive and become encapsulated by a collagenous fibrotic material from the mesenchymal cells (O'Brien et al., 2010), a process which is impaired in an *Igfbp5*-knockout mouse (Ning et al., 2007). This process ensures that residual ductal tissue is not disrupted by fibrotic tissue and thus aids in the survival of the basic ductal tree destined to develop during subsequent pregnancies (O'Brien et al., 2010). This encapsulation process is also reminiscent of the host response to tumours where the 'normal' tissue surrounding the tumour expresses proteins that belong to a 'wound-healing signature', including increased expression of collagen, fibronectin and IGFBP5 (Akkiprik et al., 2008). Thus, although

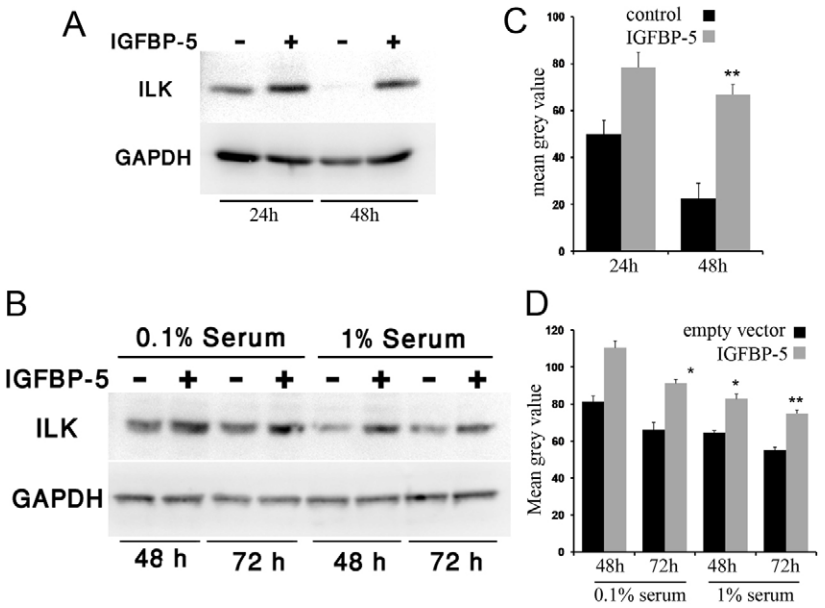

Fig. 6. ILK expression in IGFBP5 treated MCF-7 cells. (**A**) Western blotting analysis of MCF-7 cells seeded in serum-free medium and treated with 10 μg/ml exogenous IGFBP5 for 24 or 48 hours. (**B**) Western blotting analysis of Ad-IGFBP5 (200 MOI) or Ad-null transfected MCF-7 cells cultured in low serum concentrations. Cells were harvested in lysis buffer and cell lysates were immunoblotted with anti-ILK and re-probed with anti-GAPDH antibodies. (**C**,**D**) Quantitative analysis of blots normalised with GAPDH blots. Values are mean+s.e.m. of three independent blots. $*P<0.05$, $**P<0.01$ compared with control (ANOVA followed by Bonferroni's post-hoc test).

increased IGFBP5 expression has been associated with poor prognosis during metastasis (Pekonen et al., 1992; McGuire et al., 1994; Huynh, 1998; Mita et al., 2007) this might actually reflect the host response that attempts to limit metastasis. Consistent with this, IGFBP5 expression has recently been shown to be associated with increased survival times in breast cancer patients (Ahn et al., 2010). In addition, overexpression of IGFBP5 in MCF-7 xenografts inhibited tumour development in mice (Ahn et al., 2010), and recent studies have demonstrated a tumour suppressor role for IGFBP5 in osteosarcoma (Su et al., 2011) and in breast cancer after foetal alcohol exposure (Polanco et al., 2010).

Further support for a role of IGFBP5 as an anti-metastatic factor comes from studies demonstrating that IGFBP5 is one of the major secreted products of the senescence-messaging secretome (SMS), which plays an important tumour suppressor role (Adams, 2009). In addition, IGFBP5 stimulates laminin γ1 synthesis in mesangial cells, a process which would serve to better define the epithelial compartment (Abrass and Hansen, 2010) and, in this study, we showed that IGFBP5 treatment maintains E-cadherin expression, which also serves to inhibit metastasis (Makrilia et al., 2009).

Although IGFBPs influence the actions of IGFs, they also have IGF-independent actions (Beattie et al., 2006). To assess this possibility, we generated three mutant forms of IGFBP5 (Allan et al., 2006). These mutants unequivocally demonstrated that the action of IGFBP5 on cell adhesion was IGF-independent, that the activity is evident in a C-terminal fragment and that the heparin-binding domain (also in the C-terminal domain) is critical for this action. The heparin-binding domain has previously been implicated in a number of the actions of IGFBP5 (Beattie et al., 2006). By contrast, the effects of IGFBP5 on migration were again IGF-independent and also required the heparin-binding domain, but the mutant comprising only the C-terminus

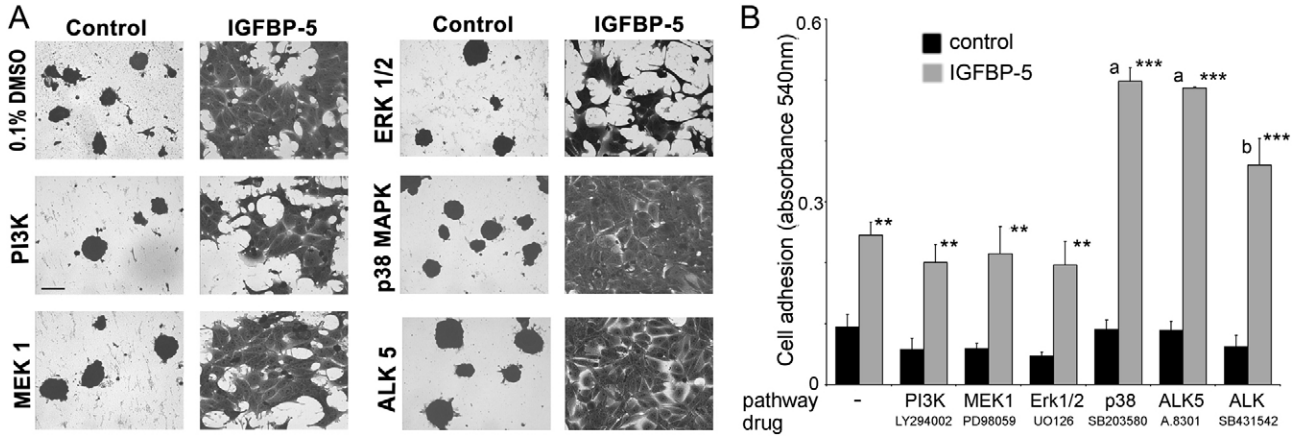

Fig. 7. Effect of kinase inhibitors on adhesion induced by IGFBP5. MCF-7 cells (3×10^4 cells per well) were cultured in the presence or absence of IGFBP5 (10 μg/ml) and various kinase inhibitors (see Materials and Methods for concentrations). After 18 hours, cells were fixed, stained with Crystal Violet and photographed (**A**) and the absorbance determined at 540 nm (**B**). Values are means+s.e.m. ($n=5$). $**P<0.01$, $***P<0.001$ compared with control. $^aP<0.01$, $^bP<0.05$ compared with IGFBP5 in the absence of drug (ANOVA followed by Bonferroni's post-hoc test). Scale bar: 50 μm.

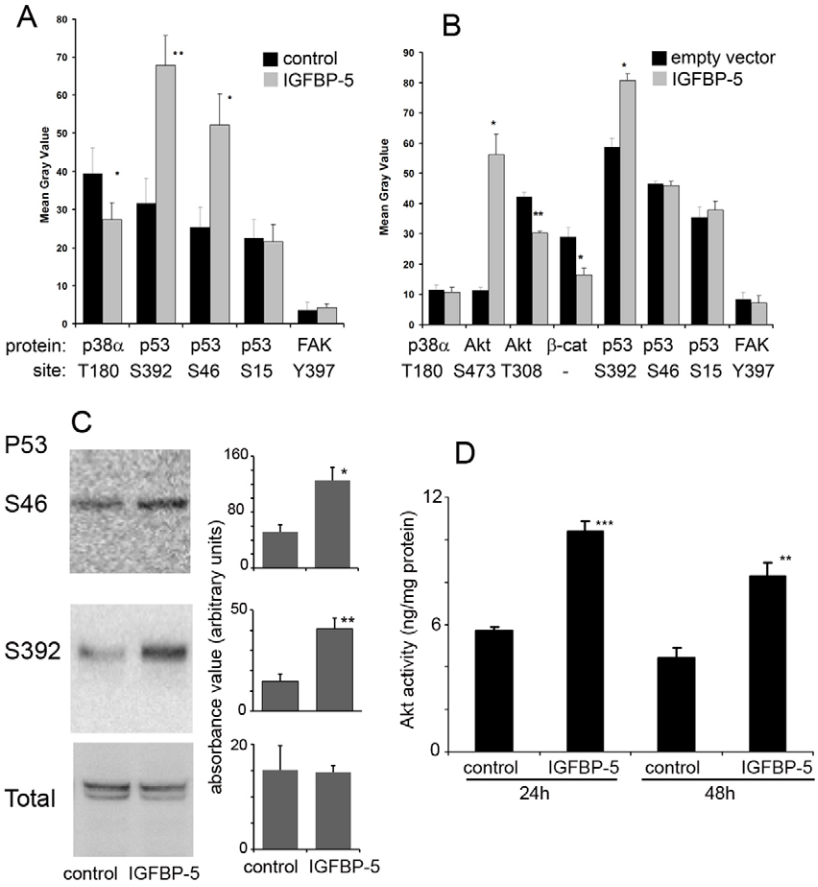

Fig. 8. Effects of IGFBP5 on kinase phosphorylation. MCF-7 cells were cultured in the presence or absence of exogenous IGFBP5 (10 μg/ml) for 6 hours (**A**) or transfected with Ad-IGFBP5 for 48 hours (**B**) after which cells were lysed. Protein concentrations were determined and 250 μg were loaded onto phosphokinase arrays, which were conducted exactly according to the manufacturer's instructions. Conventional western blotting was also performed for p53 (**C**). Blots were developed using an ECL plus detection system and quantified using Image J software. Values are mean+s.e.m. gray values (n=4). *P<0.05, **P<0.01 (ANOVA followed by Bonferroni's post-hoc test). (**D**) MCF-7 cells were cultured in the presence or absence of exogenous IGFBP5 (10 μg/ml) for 24 or 48 hours after which cell homogenates were analysed for Akt activity as described in the Materials and Methods. Values are means+s.e.m. (n=5). **P<0.01, ***P<0.001 compared with control (ANOVA followed by Bonferroni's post-hoc test).

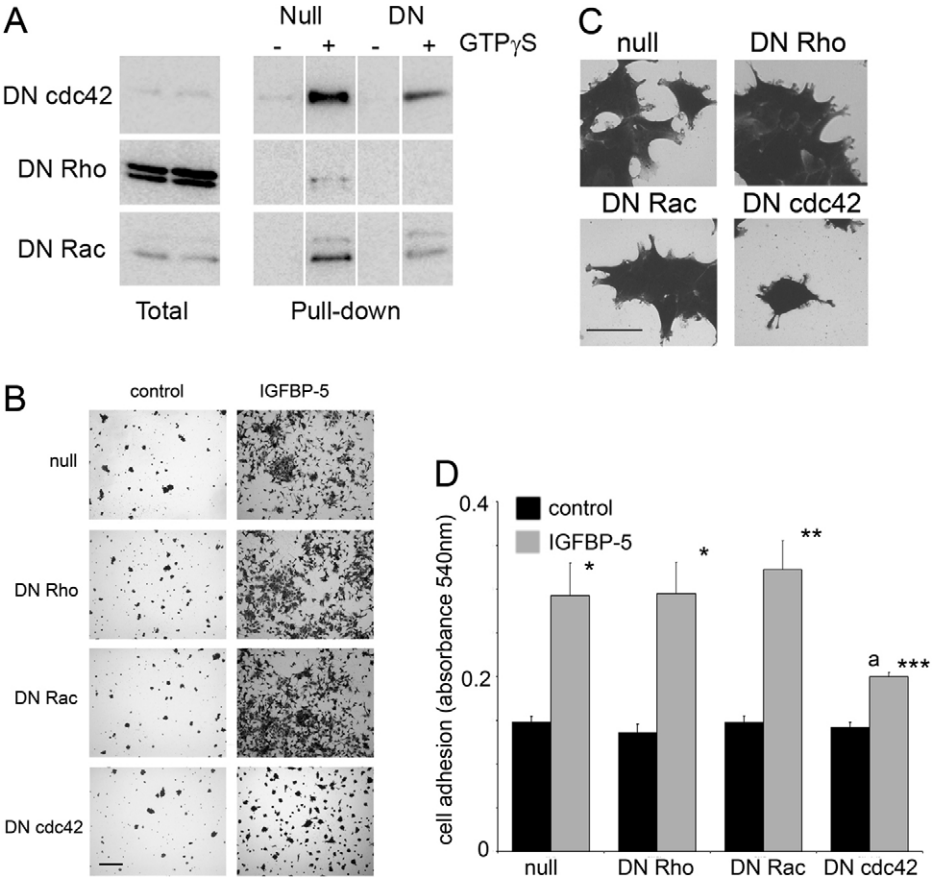

Fig. 9. Role of small GTPases in the adhesive effects of IGFBP5. MCF-7 cells were transfected with dominant negative (DN) Rho, Rac, Cdc42 or null (control) adenovirus at 200 MOI. The success of infection, was demonstrated by in vitro activation of small GTPases using GTPγS (included in the kit), followed by Rho, Rac or Cdc42 activation assays, which were performed according to the manufacturer's protocols. This clearly demonstrated inhibition of activation of all three GTPases by the respective DN construct (**A**). (**B**) DN Cdc42 but not DN Rho or DN Rac inhibited the adhesive action of IGFBP5. Transfected cells were cultured in 0.1% BSA in DMEM in the presence or absence of IGFBP5 (10 μg/ml) for 18 hours before the cells were fixed stained with Crystal Violet, photographed and absorbances determined. (**C**) Higher power (40× objective) images of IGFBP5-treated cells. (**D**) Quantitative analysis of Crystal Violet staining. Values are mean+s.e.m. gray values (n=4). *P<0.05, **P<0.01, ***P<0.001 compared with null virus. [a]P<0.01 compared with IGFBP5 response in cells treated with null virus (ANOVA followed by Bonferroni's post-hoc test). Scale bars: 100 μm (A), 50 μm (C).

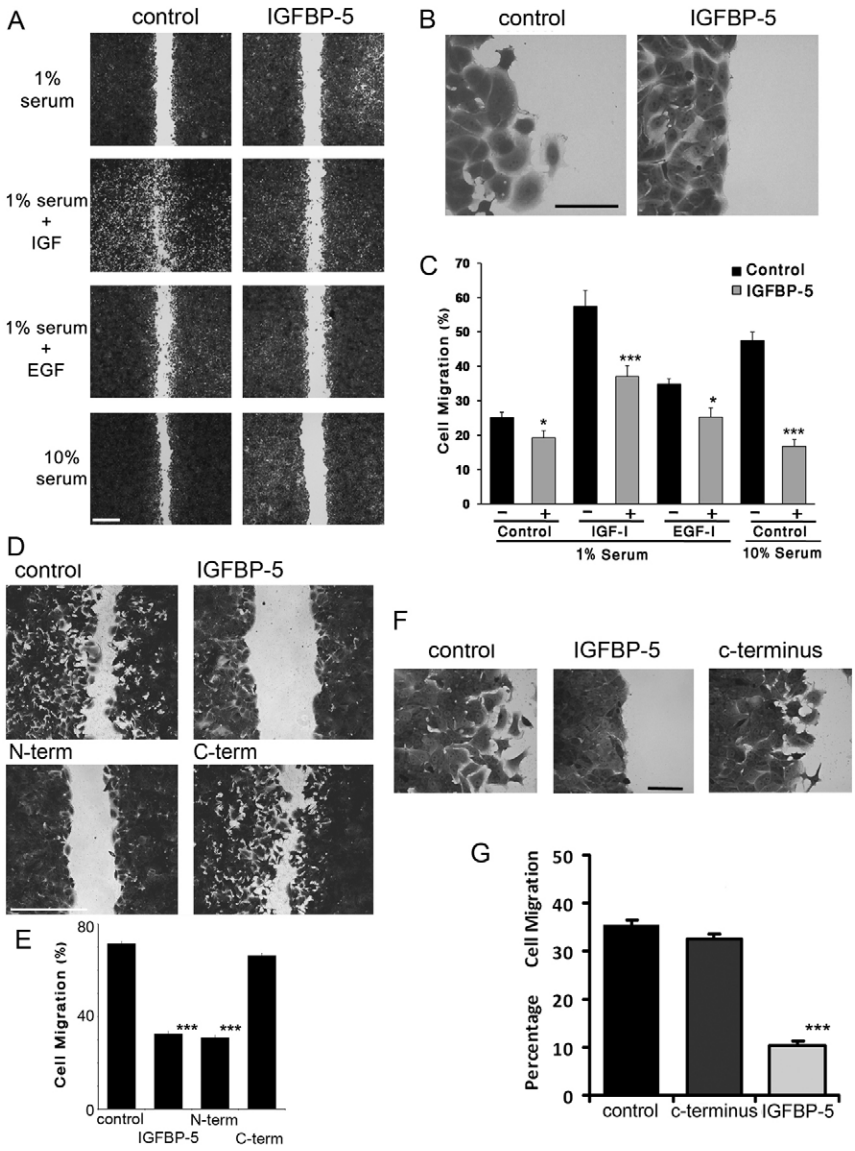

Fig. 10. IGFBP5 inhibits migration of MCF-7 cells independent of its ability to bind to IGFs. MCF-7 cells were grown in ibidi migration chambers. After washing, cells were subjected to various treatments as indicated, in the presence or absence of 10 μg/ml IGFBP5 (**A**–**C**). IGF1, EGF and serum increased cell migration, and IGFBP5 inhibited this in all cases. Migration was also assessed in the presence of 10% serum in the presence or absence of 10 μg/ml of wild-type IGFBP5, a mutant which could not bind IGFs (N-term) or a mutant which could not bind to heparin (C-term) (**D**,**E**). Finally, migration was assessed with 10% serum in the presence or absence of 10 μg/ml of wild-type IGFBP5 or 10 μg/ml of the C-terminus of IGFBP5 (**F**,**G**). Quantitative analysis of wound closure was performed after staining with Crystal Violet using ImageJ software (C,E,G). Values are mean+s.e.m. (n=3–4). *P<0.05, ***P<0.001 compared with control (ANOVA followed by Bonferroni's post-hoc test). Scale bars: 500 μm (A), 50 μm (B), 500 μm (D), 50 μm (F).

(containing an intact heparin-binding domain) failed to inhibit migration. These results suggest that both the N- and C-termini are required for inhibition of migration.

The mechanism of action of IGFBP5 has been the subject of much debate (Beattie et al., 2006). We demonstrate, for the first time, that cell adhesion stimulated by IGFBP5 is dependent upon α2β1 integrin and, furthermore, that there is a direct high-affinity interaction between IGFBP5 and α2β1 integrin. Consistent with an integrin-mediated action of IGFBP5, we demonstrated increased ILK expression, activation of Akt by phosphorylation on S473 (typical of an integrin-mediated activation) (Persad et al., 2000; Wang and Basson, 2009) and increased Akt activity after IGFBP5 treatment. This contrasts with the IGF-mediated phosphorylation of Akt on S308, a target of PI3K. Actions of IGFBP3 have also been proposed to be dependent on β1 integrin, although the mechanism involved has not been described (Burrows et al., 2006). Thus we show for the first time a direct interaction of IGFBP5 and α2β1 integrin, which leads to activation of Akt.

In contrast to its effect on cell adhesion, the action of IGFBP5 on migration did not appear to reside exclusively in the C-terminus because, although a mutant IGFBP5 that could not bind to heparin failed to influence migration, a mutant representing the C-terminus with an intact heparin-binding domain was also unable to influence migration, even though it could induce adhesion. These results suggest that the heparin-binding domain is necessary but not sufficient to inhibit migration, perhaps indicating that this process requires IGFBP5 binding to the ECM (through its heparin-binding domain) as well as to cell surface integrins, presumably through a different domain of the molecule. This proposal will require a systematic study of the interactions of IGFBP5 with α2β1 integrin.

IGFBP5 thus appears to act in similar fashion to the secreted CCN (cysteine-rich) protein family, which includes connective tissue growth factor (CTGF), cysteine-rich heparin-binding protein 61 (CYR61) and Nov (CCN3), which exert effects indirectly by interaction with integrins, growth factors and the ECM through integrin- and ECM-binding domains (Leask and

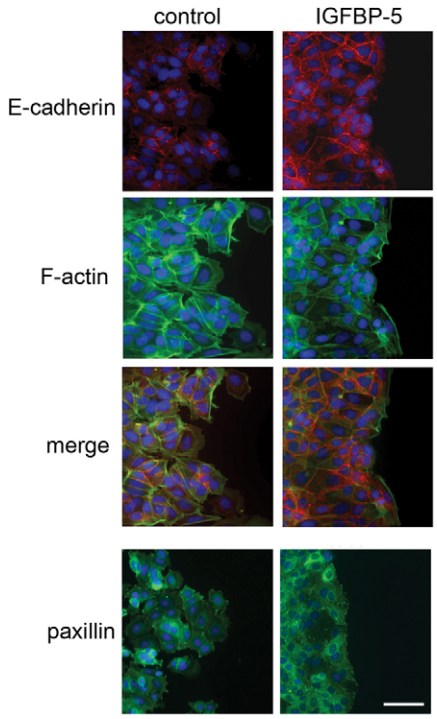

Fig. 11. Expression of E-cadherin, F-actin and paxillin in MCF-7 cells at the wound edge. Cells were examined 24 hours after wounding. E-cadherin expression (red) was downregulated close to the wound edge in control cells but maintained to within one cell of the wound edge in IGFBP5-treated cells. Nuclei were stained with DAPI (blue). F-actin (green) rearrangement was evident in control cells because lamellipodia formed. By contrast, cells treated with IGFBP5 maintained F-actin in a peripheral location, such that it superimposed with E-cadherin except where F-actin was also retained at the peripheral edge of the wound (merge). Both control and IGFBP5-treated cells possessed numerous focal adhesions as judged by paxillin expression (green). Scale bar: 50 μm.

Abraham, 2006). The CCN family are structurally related to the IGFBPs and were actually temporarily renamed IGFBP8–10. It might now be more appropriate to consider IGFBP5 as a member of the CCN family, because we now show that IGFBP5 has high-affinity integrin-binding properties, and its interactions with the ECM are well established (Beattie et al., 2006), including our recent finding that IGFBP5 interacts with the cell-binding domain of fibronectin (Beattie et al., 2009). Because turnover of integrins is essential for cell migration, it is tempting to speculate that IGFBP5 might interact simultaneously with α2β1 integrins and with ECM components such as heparan sulphate proteoglycans, fibronectin and/or collagen (Jones et al., 1993; Arai et al., 1994), thereby stabilising the complex, inhibiting integrin turnover and limiting migration potential. Furthermore, our observations suggesting that IGFBP5 enhances binding of MCF-7 cells to vitronectin in an α2β1-integrin-dependent but an αVβ3 (vitronectin receptor)-independent fashion, is best explained by the ability of IGFBP5 to bind to both α2β1 integrins (our study) and vitronectin (Kricker et al., 2003). Thus IGFBP5 might induce MCF-7 cells to bind to vitronectin despite the fact that they express almost no αVβ3 integrin. Examination of the ability of IGFBP5, α2β1 integrins and ECM proteins to form stable tripartite complexes would add further weight to this proposed mechanism, and we have already performed such studies to examine the simultaneous interactions of IGFBP5 with IGF1 and heparin (Beattie et al., 2005). Given the inhibitory effect of IGFBP5 on cell migration, the decrease in the levels of α5β1 integrin (fibronectin receptor) induced by IGFBP5 shown in this study, might also contribute to limiting migration (White et al., 2007).

Activation of Akt is an important survival signal and, when cells were cultured in serum- or nutrient-deprived conditions, IGFBP5 treatment significantly extended cell survival. This would be advantageous during tissue remodelling when vasculature is typically disrupted, hypoxia is common and nutrient supply is poor. In support of such a role for IGFBP5 in vivo, its expression is increased in the brain during hypoxia (O'Donnell et al., 2002), in Crohn's disease (Zimmermann et al., 1997) and in atherosclerotic plaques (Kim et al., 2007). In addition to enhancing cell survival, activation of Akt has also been associated both with proliferation signals and activation of FAK, which, in turn, increases migratory potential. However, in agreement with studies in human umbilical vein endothelial cells (Kim et al., 2007), we showed that IGFBP5 induced a sustained phosphorylation of p53 in MCF-7 cells, and p53, in turn, has been shown to inhibit phosphorylation of FAK (Golubovskaya et al., 2008). We thus propose that activation of p53 by IGFBP5 helps prevent migration of MCF-7 cells by inhibiting FAK phosphorylation. This mode of action has also been suggested for IGFBP3 (Perks and Holly, 1999). The expression of a mutant (inactive) form of p53 leads to an accelerated integrin turnover and increased cell migration (Muller et al., 2009). Taken together, these observations suggest that activation of wild-type p53 inhibits integrin turnover and decreases cell migration. Clearly these linkages require further study.

Despite decreased migration, focal adhesions were abundant in cells at a wound edge after IGFBP5 treatment. However, there was very limited actin re-arrangement, in contrast to in control cells, where lamellipodia and prominent actin stress fibres were evident. These findings suggest that IGFBP5 inhibits either Rac and/or Rho, which are involved in these processes.

Although we have presented evidence for a novel integrin-mediated mechanism of action for IGFBP5, IGFBP5 also inhibited phosphorylation of p38 MAPK, and the actions mediated by IGFBP5 were attenuated by activation of both the p38 MAPK and Smad pathways. This is in contrast to other p38-MAPK-dependent actions of IGFBP5, and the ability of IGFBP5 to activate the p44 (MAPK3) and p42 (MAPK1) MAPK (Kuemmerle and Zhou, 2002; Amaar et al., 2005; Yasuoka et al., 2009). Such differences might reflect differences in cell types and will require further studies to resolve the issue. Adhesion induced by IGFBP5 is dependent upon the small GTPase Cdc42 rather than Rho or Rac (Nobes and Hall, 1995; Krugmann et al., 2001). A similar, Cdc42-dependent, stimulation of adhesion by IGFBP5 has been described in neuronal cells (Berfield et al., 2000; Abrass and Hansen, 2010).

In summary, we have described a new integrin-mediated Cdc42-dependent cell survival pathway, induced by IGFBP5, which involves stimulation of ILK, Akt and p53 (Fig. 12). We believe that this action of IGFBP5 leads to an adhesive, anti-migratory, phenotype and, as such, IGFBP5 might play a key role in limiting metastasis (and also in wound healing) by restricting fibrosis to the mesenchymal compartment and preventing transgressions into, and out of, the epithelium.

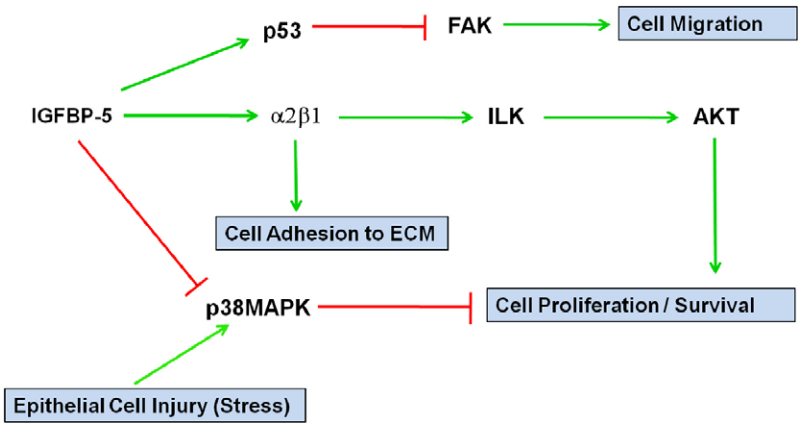

Fig. 12. Schematic representation of the actions of IGFBP5 on MCF-7 cells. Green arrows represent stimulation and red arrows represent inhibition.

Materials and Methods

Cell culture

MCF-7 breast cancer cells were maintained in Dulbecco's modified Eagle's medium (DMEM) containing 10% FBS, 2 mM L-glutamine, 100 U/ml penicillin and 100 μg/ml streptomycin at 37℃ in a 5% CO_2 atmosphere.

Production of recombinant wild-type and mutant IGFBP5

Wild-type, N-terminal (non-IGF binding) and C-terminal (non-heparin binding) mutants of IGFBP5 were produced as described previously (Allan et al., 2002). To produce the C-terminal domain of IGFBP5, the full-length cDNA encoding rat IGFBP5 in pGEM-*7zf* (Promega, Madison, WI), containing both initiator and signal peptide, was kindly provided by Sean Guenette (John Wayne Cancer Institute, Los Angeles, CA). The rat and mouse protein sequences of IGFBP5 differ by a single amino acid at position 188 (Asp and Glu, respectively). Site-directed mutagenesis was employed to convert wild-type rat into wild-type mouse sequences (D188E) as described previously (Shand et al., 2003) using the QuikChange system (Stratagene, La Jolla, CA) following the protocol provided by the manufacturer. This was then subcloned without signal peptide sequence into the pGEX 6P-1 vector (Amersham Biosciences) for bacterial expression, producing recombinant proteins with an N-terminal glutathione transferase (GST) tag. Conditions for expression, removal of tag and purification of IGFBP5 proteins were as described previously (Allan et al., 2002).

The mutant comprising only the C-terminal domain of IGFBP5 was created as follows. Site-directed mutagenesis of the wild-type IGFBP5 clone in pGEX 6P-1 was employed to introduce a *Bam*H1 restriction endonuclease site at the junction of the central and C-terminal domains of IGFBP5 (position 552 in the nucleotide sequence of the rat *Igfbp5* coding sequence). The oligonucleotides used for mutagenesis were 5′-CCTGAGATGAGACAGGGATCCGAACAAGGCCCCTG-CC-3′ and 5′-GGCAGGGGCCTTGTTCGGATCCCTGTCTCATCTCAGG-3′ respectively. The oligonucelotides were synthesised by MWG BioTech (Ebersberg, Germany) and the correct mutation was confirmed by restriction endonuclease digestion followed by automated DNA sequencing (Lark Technologies, Takeley, UK). This created a construct that had a unique *Bam*H1 restriction site within the pGEX 6P-1 sequence, between the GST tag and the *Igfbp5* cDNA, and a second *Bam*H1 site within the *Igfbp5* sequence. Following this, restriction digest with *Bam*H1 dropped out a fragment containing the N-terminal and central domains of IGFBP5, and subsequent re-ligation of the vector kept the open reading frame between the GST tag and remaining C-terminal domain of IGFBP5. Bacterial expression with this new vector, followed by tag removal, resulted in a 67-amino-acid protein (residues 185–252) with a theoretical molecular mass of 7984 Da.

Cell adhesion – effects of IGFBP5 mutants

Various concentrations of IGFBP5 (wild type, N-term and C-term mutants) and IGF1 were prepared in 0.1% BSA in DMEM. The treatments were added to 96-well plates. 3×10^4 MCF-7 cells, also in 0.1% BSA in DMEM, were added to each well in triplicate. Plates were then cultured for 24 hours at 37℃ in a 5% CO_2 atmosphere after which the medium was removed and cells were fixed with 100 μl of 4% (w/v) paraformaldehyde (PFA) in PBS for 20 minutes at room temperature, After staining with Crystal Violet, the absorbance was determined at 540 nm.

Adenoviral transfection with IGFBP5

Wild-type IGFBP5 was cloned between the *Eco*R1and *Hin*dIII sites of the Shuttle plasmid pDC516 (AdMax™, Microbix Biosystems Inc., Ontario, Canada) containing the murine cytomegalovirus immediate early gene promoter (MCMV Pr). The shuttle plasmids were then co-transfected with the adenoviral genomic plasmid (pBHGtrtΔE1,3FLP) into HEK 293 cells to employ FLP-mediated site-specific recombination between the two plasmids, resulting in recombinant, non-replicative, adenovirus (Ad-IGFBP5). All procedures used were those recommended by the manufacturer in their Ad Vector Construction Manual (Microbix Biosystems Inc.). Adenoviral stocks were generated commercially and a null virus was purchased from the same source (Welgen Incorporation, Worcester, MA).

Cell adhesion assays using adenovirally transfected IGFBP5

MCF-7 cells were transfected with Ad-IGFBP5 at a multiplicity of infection (MOI) of 200 and seeded at 50,000 cells per ml or 500,000 cells per ml in 96-well plates in 10% FCS in DMEM (prepared in house). Control cells received adenovirus containing no construct (empty vector). Cells were cultured with various concentrations of serum and/or 100 ng/ml IGF1. Thereafter, cultures were maintained without medium changes and stopped at various time points. Cells were also seeded at low and high seeding density in the presence or absence of exogenous IGFBP5 in serum-free conditions. At various intervals, the reagent WST-1 was used to measure metabolic activity and cells were analysed for cell viability using live/dead or viability/cytotoxicity kits (catalogue no. L3224; Invitrogen Molecular Probes). After washing cells twice in serum-free medium, both empty vector and IGFBP5-transduced MCF-7 cells were incubated with Live/Dead stain for 15 minutes at room temperature. Live and dead fluorescence absorbances were determined at excitation and emission wavelengths of 495 nm and 517 nm (calcein), and 528 nm and 617 nm (ethidium bromide), respectively. Cells were also stopped and fixed using 4% PFA for staining with Crystal Violet and photographed. Absorbance values were determined spectrophotometrically at 540 nm.

Adenoviral transfection with DN Rho, Rac and Cdc42

Recombinant adenoviruses coding for dominant-negative mutants of Rho (RhoA T19N), Rac (Rac1 T17N) Cdc42 (Cdc42 T17N), and null control adenovirus were purchased from Cell Biolabs. MCF-7 cells were detached with 2 mM EDTA and washed twice with serum-free DMEM. 1×10^6 cells were seeded in 5 ml of DMEM containing 0.1% BSA in 10-cm dishes or 75-cm^2 flasks. Null, DN-Rho, DN-Rac or DN-Cdc42 adenovirus vectors were added at an MOI of 200. After incubation for 3 hours, 0.5 ml of serum was added to the cells, and incubation continued for 3–4 days. The infected cells were then trypsinised and washed three times with serum-free DMEM. Cells were seeded at 2×10^4 cells per well in 96-well plates in the presence or absence of 10 μg/ml IGFBP5 for 24 hours. Cells were then fixed and stained with Crystal Violet, photographed and the absorbance determined.

Rho, Rac and Cdc42 activation assay

Rho assay reagent (Upstate) and the Cdc42 activation assay kit (for Rac and Cdc42 activity, Upstate) were used to analyze Rho, Rac and Cdc42 activity as described previously (Taylor and Shalloway, 1996). In vitro activation of small GTPases using GTPγS (included in the kit) and Rho, Rac and Cdc42 activation assays were performed according to the manufacturer's protocols. Briefly, MCF-7 cells infected in a 10-cm dish and were lysed with 500 μl of lysis buffer. Cell lysates were separated into four tubes containing 100 μl of lysate. Half of the lysates were treated with 100 μM GTPγS. GTP-bound active forms of Rho, Rac and Cdc42 were collected by pull down with photekin or PAK1, subjected to SDS-PAGE, and then probed with anti-Rho, Rac or Cdc42 antibodies, respectively.

Cell signalling studies

Inhibition assays

Inhibitors were added to 96-well plates containing 3×10^4 MCF-7 cells in 0.1% BSA in DMEM in the presence and absence of IGFBP5 and cultured for 24 hours, after which cells were fixed and stained with Crystal Violet. Final concentrations

of the inhibitors used were LY-294002 (5 μM), PD98059 (25 μM), SB 203580 (1 μM), UO126 (10 μM), A83.01 (10 μM) and SB431542 (10 μM). Control wells contained an equivalent concentration of DMSO.

Phospho-kinase arrays

A human phospho-kinase array kit (R&D Systems; catalogue no. ARY003) was used to analyse 46 serine/threonine phosphorylation sites on 37 different proteins (see http://www.rndsystems.com/product_detail_objectname_kinaseantibodyarray.aspx for the complete list). MCF-7 cells seeded at 10^6 cells/ml, in triplicate, in 6-well plates were treated with exogenous IGFBP5 or by adenoviral transfection with IGFBP5. After treatment, cells were lysed at 6 or 48 hours. Cellular extracts were prepared and kinase array blots incubated with 250 μg of total protein in accordance with the manufacturer's instructions. All the blots were developed with an ECL plus western blot detection system (GE healthcare) and visualised with an LAS 3000 image reader (Fuji, Dusseldorf, Germany). Mean gray values of each spot of the array were determined using Image J.

Western immunoblot analysis

Cellular protein extracts were loaded with a prestained protein mass ladder on a NuPAGE 12% Bis-Tris mini electrophoretic system. Proteins were electroblotted onto a Hybond-C extramembrane (Amersham Biosciences) for immunoblotting analysis. Non-specific binding was prevented with 3% BSA in TBS with Tween. After blocking, the membrane was incubated with primary antibodies against: human ILK at 1:2000 dilution (rabbit, ab2283, Abcam), p53 phosphorylated at serine 46 (rabbit), p53 phosphorylated at serine 392 (rabbit, Cell Signaling) and total p53 (mouse, Calbiochem) all at 1:500 dilution in blocking buffer on a shaker overnight at 4℃. The membrane was then incubated with anti-rabbit (or mouse) horseradish-peroxidise-conjugated secondary antibody (Sigma, UK) diluted 1:5000 at room temperature for 1 hour. The blot was developed with an ECL plus western blot detection system (GE Healthcare) and visualised with an LAS 3000 image reader (Fuji, Dusseldorf, Germany). To confirm equal sample loading and transfer, membranes were stripped using Reblot buffer (Thermo Scientific, Northumberland, UK), re-blocked and re-probed with an antibody against glyceraldehyde 3-phosphate dehydrogenase at 1:5000 dilution (ab9485, Abcam) Mean grey values of each spot of the array were determined using Image J and normalised to GAPDH.

Akt activity assay

Akt activity was assayed using the K-LISA™ Akt Activity Kit (Calbiochem) according to the manufacturer's instructions. It is an ELISA-based activity assay which utilizes a biotinylated peptide substrate (GRPRTSSFAEG) that is phosphorylated on the second serine by Akt1, Akt2, Akt3, SGK (Serum Glucocorticoid Kinase), and MSK1. Biotinylated Akt substrate and samples containing Akt were incubated in the presence of ATP in wells of a streptavidin-coated 96-well plate, to allow for phosphorylation and substrate capture in a single step. The phosphorylated substrate was detected with a phosphoserine detection antibody, followed by an HRP-Antibody Conjugate and colour development with TMB Substrate. The activity was determined by reading the absorbance at dual wavelengths 450/540 nm or 450/595 nm and comparing these to an activated Akt standard.

α- and β-integrin-mediated cell adhesion array

An Avanticell cell adhesion kit was used, containing microtiter strips pre-coated with mouse monoclonal antibodies against human α (α1, α2, α3, α4, α5, αV and αVβ3) and β (β1, β2, β3, β4, β6, αVβ5 and α5β1) integrins and/or integrin subunits, along with a negative control. Each well was washed with 300 μl of wash buffer I (provided in the kit). MCF-7 cells were cultured overnight in the presence or absence of IGFBP5 and were then trypsinised and washed in serum-free medium. Cells were counted and adjusted to 4×10^5 cells/ml, added to the integrin-binding strips and incubated for 3 hours at 37℃ in a 5% CO_2 atmosphere. Wells were then emptied by inversion, washed three times with 200 μl of wash buffer II, incubated with 100 μl of cell stain solution for 10 minutes followed by further washes to remove unbound stain. Stain release solution was used to release the dye and the absorbance read at 540 nm.

Calculations

The values obtained for the negative wells were subtracted from those containing antibodies to determine specific binding.

Effect of function-blocking integrin antibodies on MCF-7 cell adhesion

3×10^4 MCF-7 cells were added to wells containing 5 μg/ml of antibodies to integrins in the presence or absence of 10 μg/ml of IGFBP5 in 0.1% BSA in DMEM. Function-blocking antibodies used were against β1 (MAB1987Z), αVβ6 (MAB2077Z), αVβ3 (MAB1976Z), αVβ5 (MAB1961Z) α2 (MAB1950Z), and α5 (MAB1956Z) (all from Chemicon International, California). Plates were incubated for 24 hours at 37℃ in a 5% CO_2 atmosphere before fixation and staining with Crystal Violet. They were then photographed and the dye solubilised using 0.1% Triton X-100. Absorbance values were determined spectrophotometrically at 540 nm. In addition, a β1-integrin-activating antibody (KM16, Abcam) was also assessed in the absence and presence of IGFBP5 in identical fashion.

Immunofluorescence staining

MCF-7 cells were cultured for 24 hours in the absence or presence of 10 μg/ml of IGFBP5 in wells of a chamber slide. As a positive control, cells were also cultured with 10% FCS in DMEM. After 24 hours, medium was removed from the wells by inverting the chamber slides and cells were fixed with 200 μl of 2% (w/v) paraformaldehyde in PBS for 10 minutes followed by permeabilisation with 200 μl of 0.5% Triton X-100 in PBS for 15 minutes at room temperature. Non-specific staining was diminished by incubating with 10% heat-inactivated (HI) serum from the species in which the second antibody was produced. Cells were incubated with 200 μl of antibodies against mouse anti-human E-cadherin (5 μg/ml) (catalogue no. 610181, BD Biosciences) or 200 μl of a 1:250 dilution of rabbit anti-human-paxillin antibody (product no. ab32084, Abcam) at 4℃ overnight. This was followed by a 1-hour incubation with respective secondary antibody and with Rhodamine–phalloidin (catalogue no. 610181, Biotium) to stain F-actin at 37℃. Slides were stained with antifade DAPI nucleic acid mountant (Molecular Probes, Invitrogen). The slides were visualised with a Nikon TE300 inverted epifluorescence microscope using ×40 or ×100 objectives with oil immersion and a Hamamatsu CCD camera (Hammamatsu Photonics, Welwyn Garden City, Hertfordshire, UK) controlled by Metamorph software (Molecular Devices, Palo Alto, CA) or a Leica DMIRB microscope using a ×40 objective (Leica N PLAN 40×, 0.55 NA CORR PH2 0-2/C), a ×10 objective (Leica N PLAN 10×, 0.25 PH1 -/A 5.8) or a ×5 objective (Leica N PLAN 5×/0.12 PH0 -/A). Images were captured on a Leica DC200 (DMIRB) and analysed using a Leica Q550 Image Analysis Workstation (v. 2.2.1) combined with Leica Qwin Software for image acquisition.

Biosensor data analysis

Human IGFBP5 (product no. 875-B5-025) and human α2β1 integrin (product no. 5698-A2-050) were both from R&D Systems. All other reagents for Biosensor analysis were obtained from GE Healthcare. Biosensor analysis was performed on a Biacore 3000 SPR instrument as described previously (Beattie et al., 2005). Recombinant human IGFBP5 was immobilised onto the surface of a CM5 biosensor chip as described previously (Beattie et al., 2008) at a substitution level of ~4000 reflectance units (RUs). α2β1 integrin binding was analysed by random injection in duplicate at concentrations of 0, 0.625, 1.25, 2.5, 5 and 10 nM. The control flow cell contained BSA immobilised at a similar level to human IGFBP5 and the response to BSA was subtracted automatically from sensorgrams. The buffer flow rate was 30 μl/minute, with a 5-minute association phase and 15-minute dissociation phase. Regeneration of the IGFBP5 surface was achieved with two 30-second pulses of 0.1% SDS. Duplicate controls containing zero analyte were also subtracted from sensorgrams. For comparisons of wild-type and mutant forms of IGFBP5, binding to a constant amount (10 nM) of α2β1 integrin was determined in replicate samples ($n=7$).

Migration assays

The cell migration assay was carried out in 24-well plates using ibidi 2-chamber inserts (Thistle Scientific Ltd, Glasgow, UK). Chambers were added to the wells and then seeded with, typically 30,000–50,000 cells to achieve a confluent monolayer overnight. Treatments were also added at this time. After overnight culture the inserts were removed to reveal to patches of cells separated by a 500 μm gap. Fresh medium containing treatments was added and migration allowed to proceed. Migration was stopped by fixing in 4% PFA. Cells were stained with Crystal Violet and images taken for analysis using ImageJ software.

Preparation of samples for SuperArray PCR

MCF-7 cells were infected with Ad-CMV-Null or Ad-IGFBP5 adenovirus at an MOI of 1000 and total RNA was extracted using Qiagen RNAeasy Mini kit (catalogue no. 74134). First strand cDNA synthesis was performed using 1 μg of RNA and an RT^2 first strand kit (SA Biosciences, catalogue no. C-03) according to the manufacturer's instructions. Gene expression profiling was performed using human ECM and adhesion molecules from the RT^2 Profiler™ PCR array system (PAHS-013C, SA Biosciences).

The PCRs were performed using an Applied Biosystems 7500 Fast Real-Time PCR System with the recommended program. Threshold cycle points (Ct) were calculated using Applied Biosystems 7500 Fast System SDS software (v. 1.3.1) after manually setting baseline and threshold values. Fold changes in gene expression were calculated (http://www.sabiosciences.com/pcr/arrayanalysis.php) after normalising data with the average Ct of the five housekeeping genes in the array.

Statistical analysis

Data were analysed using analysis of variance followed by Bonnferroni's post-hoc test.

Acknowledgements

We thank Jo-Ann Smith for expert technical assistance.

Funding

This research was funded by the Biotechnology and Biological Sciences Research Council [grant number BB\F00205X\1], Rural and Environment Research and Analysis Directorate (UK) and the University of Strathclyde.

References

Abrass, C. K. and Hansen, K. M. (2010). Insulin-like growth factor-binding protein-5-induced laminin gamma1 transcription requires filamin A. *J. Biol. Chem*. **285**, 12925-12934.

Adams, P. D. (2009). Healing and hurting: molecular mechanisms, functions, and pathologies of cellular senescence. *Mol. Cell* **36**, 2-14.

Ahn, B. Y., Elwi, A. N., Lee, B., Trinh, D. L., Klimowicz, A. C., Yau, A., Chan, J. A., Magliocco, A. and Kim, S. W. (2010). Genetic screen identifies insulin-like growth factor binding protein 5 as a modulator of tamoxifen resistance in breast cancer. *Cancer Res.* **70**, 3013-3019.

Akkiprik, M., Feng, Y., Wang, H., Chen, K., Hu, L., Sahin, A., Krishnamurthy, S., Ozer, A., Hao, X. and Zhang, W. (2008). Multifunctional roles of insulin-like growth factor binding protein 5 in breast cancer. *Breast Cancer Res*. **10**, 212-225.

Allan, G. J., Tonner, E., Barber, M. C., Travers, M. T., Shand, J. H., Vernon, R. G., Kelly, P. A., Binart, N. and Flint, D. J. (2002). Growth hormone, acting in part through the insulin-like growth factor axis, rescues developmental, but not metabolic, activity in the mammary gland of mice expressing a single allele of the prolactin receptor. *Endocrinology* **143**, 4310-4319.

Allan, G. J., Tonner, E., Szymanowska, M., Shand, J. H., Kelly, S. M., Phillips, K., Clegg, R. A., Gow, I. F., Beattie, J. and Flint, D. J. (2006). Cumulative mutagenesis of the basic residues in the 201-218 region of insulin-like growth factor (IGF)-binding protein-5 results in progressive loss of both IGF-I binding and inhibition of IGF-I biological action. *Endocrinology* **147**, 338-349.

Amaar, Y. G., Baylink, D. J. and Mohan, S. (2005). Ras-association domain family 1 protein, RASSF1C, Is an IGFBP-5 binding partner and a potential regulator of osteoblast cell proliferation. *J. Bone Miner. Res*. **20**, 1430-1439.

Arai, T., Arai, A., Busby, W. H., Jr and Clemmons, D. R. (1994). Glycosaminoglycans inhibit degradation of insulin-like growth factor- binding protein-5. *Endocrinology* **135**, 2358-2363.

Beattie, J., Phillips, K., Shand, J. H., Szymanowska, M., Flint, D. J. and Allan, G. J. (2005). Molecular recognition characteristics in the insulin-like growth factor (IGF)-insulin-like growth factor binding protein -3/5 (IGFBP-3/5) heparin axis. *J. Mol. Endocrinol*. **34**, 163-175.

Beattie, J., Allan, G. J., Lochrie, J. D. and Flint, D. J. (2006). Insulin-like growth factor-binding protein-5 (IGFBP-5): a critical member of the IGF axis. *Biochem. J.* **395**, 1-19.

Beattie, J., Phillips, K., Shand, J. H., Szymanowska, M., Flint, D. J. and Allan, G. J. (2008). Molecular interactions in the insulin-like growth factor (IGF) axis: a surface plasmon resonance (SPR) based biosensor study. *Mol. Cell. Biochem.* **307**, 221-236.

Beattie, J., Kreiner, M., Allan, G. J., Flint, D. J., Domingues, D. and van der Walle, C. F. (2009). IGFBP-3 and IGFBP-5 associate with the cell binding domain (CBD) of fibronectin. *Biochem. Biophys. Res. Commun*. **381**, 572-576.

Berfield, A. K., Andress, D. L. and Abrass, C. K. (2000). IGFBP-5(201-218) stimulates Cdc42GAP aggregation and filopodia formationin migrating mesangial cells. *Kidney Int.* **57**, 1991-2003.

Burrows, C., Holly, J. M., Laurence, N. J., Vernon, E. G., Carter, J. V., Clark, M. A., McIntosh, J., McCaig, C., Winters, Z. E. and Perks, C. M. (2006). Insulin-like growth factor binding protein 3 has opposing actions on malignant and nonmalignant breast epithelial cells that are each reversible and dependent upon cholesterol-stabilized integrin receptor complexes. *Endocrinology* **147**, 3484-3500.

Cance, W. G. and Golubovskaya, V. M. (2008). Focal adhesion kinase versus p53: apoptosis or survival? *Sci. Signal.* **1**, pe22.

Clarkson, R. W. and Watson, C. J. (2003). Microarray analysis of the involution switch. *J. Mammary Gland Biol. Neoplasia* **8**, 309-319.

Golubovskaya, V. M., Finch, R., Kweh, F., Massoll, N. A., Campbell-Thompson, M., Wallace, M. R. and Cance, W. G. (2008). p53 regulates FAK expression in human tumor cells. *Mol. Carcinog.* **47**, 373-382.

Hall, A. (1998). Rho GTPases and the actin cytoskeleton. *Science* **279**, 509-514.

Huynh, H. (1998). In vivo regulation of the insulin-like growth factor system of mitogens by human chorionic gonadotropin. *Int. J. Oncol.* **13**, 571-575.

Jones, J. I., Gockerman, A., Busby, W. H., Jr, Camacho-Hubner, C. and Clemmons, D. R. (1993). Extracellular matrix contains insulin-like growth factor binding protein-5: potentiation of the effects of IGF-I. *J. Cell Biol.* **121**, 679-687.

Kim, K. S., Seu, Y. B., Baek, S. H., Kim, M. J., Kim, K. J., Kim, J. H. and Kim, J. R. (2007). Induction of cellular senescence by insulin-like growth factor binding protein-5 through a p53-dependent mechanism. *Mol. Biol. Cell* **18**, 4543-4552.

Kricker, J. A., Towne, C. L., Firth, S. M., Herington, A. C. and Upton, Z. (2003). Structural and functional evidence for the interaction of insulin-like growth factors (IGFs) and IGF binding proteins with vitronectin. *Endocrinology* **144**, 2807-2815.

Krugmann, S., Jordens, I., Gevaert, K., Driessens, M., Vandekerckhove, J. and Hall, A. (2001). Cdc42 induces filopodia by promoting the formation of an IRSp53:Mena complex. *Curr. Biol.* **11**, 1645-1655.

Kuemmerle, J. F. and Zhou, H. (2002). Insulin-like growth factor-binding protein-5 (IGFBP-5) stimulates growth and IGF-I secretion in human intestinal smooth muscle by Ras-dependent activation of p38 MAP kinase and Erk1/2 pathways. *J. Biol. Chem*. **277**, 20563-20571.

Leask, A. and Abraham, D. J. (2006). All in the CCN family: essential matricellular signaling modulators emerge from the bunker. *J. Cell. Sci.* **119**, 4803-4810.

Makrilia, N., Kollias, A., Manolopoulos, L. and Syrigos, K. (2009). Cell adhesion molecules: role and clinical significance in cancer. *Cancer Invest.* **27**, 1023-1037.

Marshman, E., Green, K. A., Flint, D. J., White, A., Streuli, C. H. and Westwood, M. (2003). Insulin-like growth factor binding protein 5 and apoptosis in mammary epithelial cells. *J. Cell Sci.* **116**, 675-682.

McCaig, C., Perks, C. M. and Holly, J. M. (2002). Intrinsic actions of IGFBP-3 and IGFBP-5 on Hs578T breast cancer epithelial cells: inhibition or accentuation of attachment and survival is dependent upon the presence of fibronectin. *J. Cell Sci.* **115**, 4293-4303.

McGuire, S. E., Hilsenbeck, S. G., Figueroa, J. A., Jackson, J. G. and Yee, D. (1994). Detection of insulin-like growth factor binding proteins (IGFBPs) by ligand blotting in breast cancer tissues. *Cancer Lett.* **77**, 25-32.

Mita, K., Zhang, Z., Ando, Y., Toyama, T., Hamaguchi, M., Kobayashi, S., Hayashi, S., Fujii, Y., Iwase, H. and Yamashita, H. (2007). Prognostic significance of insulin-like growth factor binding protein (IGFBP)-4 and IGFBP-5 expression in breast cancer. *Jpn. J. Clin. Oncol.* **37**, 575-582.

Muller, P. A., Caswell, P. T., Doyle, B., Iwanicki, M. P., Tan, E. H., Karim, S., Lukashchuk, N., Gillespie, D. A., Ludwig, R. L., Gosselin, P. et al. (2009). Mutant p53 drives invasion by promoting integrin recycling. *Cell* **139**, 1327-1341.

Ning, Y., Hoang, B., Schuller, A. G., Cominski, T. P., Hsu, M. S., Wood, T. L. and Pintar, J. E. (2007). Delayed mammary gland involution in mice with mutation of the insulin-like growth factor binding protein 5 gene. *Endocrinology* **148**, 2138-2147.

Nobes, C. D. and Hall, A. (1995). Rho, rac, and cdc42 GTPases regulate the assembly of multimolecular focal complexes associated with actin stress fibers, lamellipodia, and filopodia. *Cell* **81**, 53-62.

O'Brien, J., Lyons, T., Monks, J., Lucia, M. S., Wilson, R. S., Hines, L., Man, Y. G., Borges, V. and Schedin, P. (2010). Alternatively activated macrophages and collagen remodeling characterize the postpartum involuting mammary gland across species. *Am. J. Pathol.* **176**, 1241-1255.

O'Donnell, S. L., Frederick, T. J., Krady, J. K., Vannucci, S. J. and Wood, T. L. (2002). IGF-I and microglia/macrophage proliferation in the ischemic mouse brain. *Glia* **39**, 85-97.

Pekonen, F., Nyman, T., Ilvesmaki, V. and Partanen, S. (1992). Insulin-like growth factor binding proteins in human breast cancer tissue. *Cancer Res.* **52**, 5204-5207.

Perks, C. M. and Holly, J. M. P. (1999). Insulin-like growth factor binding protein-3 (IGFBP-3) modulates the phosphorylation of focal adhesion kinase (FAK) independently of IGF in Hs578T human breast cancer cells. *Growth Horm. IGF Res*. **9**, 369.

Persad, S., Attwell, S., Gray, V., Delcommenne, M., Troussard, A., Sanghera, J. and Dedhar, S. (2000). Inhibition of integrin-linked kinase (ILK) suppresses activation of protein kinase B/Akt and induces cell cycle arrest and apoptosis of PTEN-mutant prostate cancer cells. *Proc. Natl. Acad. Sci. USA* **97**, 3207-3212.

Polanco, T. A., Crismale-Gann, C., Reuhl, K. R., Sarkar, D. K. and Cohick, W. S. (2010). Fetal alcohol exposure increases mammary tumor susceptibility and alters tumor phenotype in rats. *Alcohol Clin. Exp. Res.* **34**, 1879-1887.

Shand, J. H., Beattie, J., Song, H., Phillips, K., Kelly, S. M., Flint, D. J. and Allan, G. J. (2003). Specific amino acid substitutions determine the differential contribution of the N- and C-terminal domains of insulin-like growth factor (IGF)-binding protein-5 in binding IGF-I. *J. Biol. Chem.* **278**, 17859-17866.

Stein, T., Morris, J. S., Davies, C. R., Weber-Hall, S. J., Duffy, M. A., Heath, V. J., Bell, A. K., Ferrier, R. K., Sandilands, G. P. and Gusterson, B. A. (2004). Involution of the mouse mammary gland is associated with an immune cascade and an acute-phase response, involving LBP, CD14 and STAT3. *Breast Cancer Res.* **6**, R75-R91.

Su, Y., Wagner, E. R., Luo, Q., Huang, J., Chen, L., He, B. C., Zuo, G. W., Shi, Q., Zhang, B. Q., Zhu, G. et al. (2011). Insulin-like growth factor binding protein 5 suppresses tumor growth and metastasis of human osteosarcoma. *Oncogene* **30**, 3907-3917.

Taylor, S. J. and Shalloway, D. (1996). Cell cycle-dependent activation of Ras. *Curr. Biol*. **6**, 1621-1627.

Tonner, E., Barber, M. C., Travers, M. T., Logan, A. and Flint, D. J. (1997). Hormonal control of insulin-like growth factor-binding protein-5 production in the involuting mammary gland of the rat. *Endocrinology* **138**, 5101-5107.

Tonner, E., Barber, M. C., Allan, G. J., Beattie, J., Webster, J., Whitelaw, C. B. and Flint, D. J. (2002). Insulin-like growth factor binding protein-5 (IGFBP-5) induces premature cell death in the mammary glands of transgenic mice. *Development* **129**, 4547-4557.

Wang, S. and Basson, M. D. (2009). Integrin-linked kinase: a multi-functional regulator modulating extracellular pressure-stimulated cancer cell adhesion through focal adhesion kinase and AKT. *Cell Oncol.* **31**, 273-289.

White, D. P., Caswell, P. T. and Norman, J. C. (2007). alpha v beta3 and alpha5beta1 integrin recycling pathways dictate downstream Rho kinase signaling to regulate persistent cell migration. *J. Cell. Biol.* **177**, 515-525.

Yasuoka, H., Yamaguchi, Y. and Feghali-Bostwick, C. A. (2009). The pro-fibrotic factor iGFBP-5 induces lung Fibroblast and mononuclear cell migration. *Am. J. Respir. Cell. Mol. Biol.* **41**, 179-188.

Zimmermann, E. M., Li, L., Hou, Y. T., Cannon, M., Christman, G. M. and Bitar, K. N. (1997). IGF-I induces collagen and IGFBP-5 mRNA in rat intestinal smooth muscle. *Am. J. Physiol.* **273**, G875-G882.

Journal of Cell Science